10/695,519

STATE OF ISRAEL
מדינת ישראל

Ministry of Justice
Patent Office

משרד המשפטים
לשכת הפטנטים

This is to certify that annexed hereto is a true copy of the documents as originally deposited with the patent application of which particulars are specified on the first page of the annex.

זאת לתעודה כי רצופים בזה העתקים נכונים של המסמכים שהופקדו לכתחילה עם הבקשה לפטנט לפי הפרטים הרשומים בעמוד הראשון של הנספח.

This ___19 -01- 2004___ היום
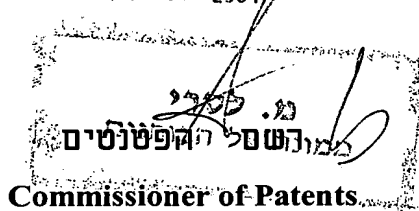
Commissioner of Patents

נתאשר
Certified

בקשה לפטנט

Application for Patent

מספר: Number	**152519**
תאריך: Date	**28 -10- 2002**
הוקדם / נדחה: Ante / Post-dated	

אני , (שם המבקש, מענו - ולגבי גוף מאוגד - מקום התאגדותו)
I (Name and address of applicant, and, in case of body corporate place of incorporation)

Civcom Devices & Systems Ltd.
2 Hagranite Street
Petach Tikva 49514
Israel

סיבקום התקנים ומערכות בע"מ
רחוב הגרניט 2
פתח תקוה 49514
ישראל

בעל אמצאה מכח _____ הדין _____ Law _____ ששמה הוא
Owner, by virtue of   Of an invention, the title of which is

(בעברית)
(Hebrew)   שיטה ומנגנון להערכה של OSNR בתוך ערוץ

(באנגלית)
(English)   A Method and Apparatus for In-Channel OSNR Estimation

מבקש בזאת כי ינתן לי עליה פטנט   Hereby apply for a patent to be granted to me in respect therof

•בקשת חלוקה - Application of Division	•בקשת פטנט מוסף - Application for Patent Addition	•דרישה דין קדימה Priority Claim		
מבקשת פטנט from Application	•לבקשה/לפטנט to Patent/Appl.	מספר/ סימן Number/Mark	תאריך Date	מדינת האגוד Convention Country
No._____ מס׳ Dated _____ מיום	No._____ מס׳ Dated _____ מיום			

•ייפוי כח (כללי/מיוחד) - רצוף בזה / עוד יוגש
P.O.A: general / individual - attached / to be filed later

filed in case ___150453___ הוגש בעניין

המען למסירת הודעות ומסמכים בישראל
Address for Service in Israel
פנסטר ושות׳
עורכי פטנטים בע"מ
רח׳ בזל 16 פ"ת
ת.ד 10256 פ"ת 49002

עבור המבקש,	חתימת המבקש Signature of Applicant	היום __28__ This בחודש __אוקטובר__ Of שנת __2002__ Of the year	לשימוש הלשכה For Office Use

פנסטר ושות׳
עורכי פטנטים בע"

298/03282

Delete whatever is inapplicable   •מחק את המיותר

שיטה ומנגנון להערכה של OSNR בתוך ערוץ

A Method and Apparatus for In-Channel OSNR Estimation

ממציאים:
זאב זלבסקי
ורדית אקהויז

Inventors:
Zeev Zalevsky
Vardit Eckhouse

A method and apparatus for In-Channel OSNR Estimation

Background of the invention

The ability to characterize the shape of optical pulses in high rate is very complicated and requires expensive electronics. However, knowing the phase and the amplitude of the pulse may be useful for predicting mitigation from optical fiber transmission impairments such as chromatic dispersion, polarization mode dispersion and non linear distortions. Techniques including direct sampling [Refs. 1-2], non-linear pulse characterization [Refs. 3-4] or other direct approaches [Refs. 5-7] have disadvantages of high price, low precision and sensitivity.

In addition, the need to extract the Optical Signal to Noise Ratio (OSNR) is very important for accurately isolating faults in the network. It can also be used to estimate the value of Amplifier Spontaneous Emission (ASE) noise and can be used for estimating the Bit Error rate (BER) or the Q factor of the incoming signal stream. Since the signal is much stronger than the noise the computation of this ratio is commonly performed in-between adjacent WDM channels. However, different WDM channels may have different levels of noise and signal since they were originated in different positions along the optical layer and in many cases, signals pass through demux or filters that filter out the wavelengths between channels. Thus, in order to evaluate the true Optical Signal to Noise Ratio (OSNR) one needs to estimate the OSNR within the channel. To succeed in this task one must develop a technique in which the signal is depressed much stronger than the noise. Several techniques to obtain this objective were published. The most common technique is the polarization nulling [Refs. 8-9] where a usage is made for the fact that the polarization of the signal varies slowly while the noise is non-polarized. A polarization controller changes the polarization state of the incoming signal such that when it is passed through a polarized beam splitter one output is the noise and the other output is the noise and the signal. However, this technique fails in the presence of Polarization Mode Dispersion (PMD) since then the Degree Of Polarization (DOP) of the signal itself is not 1. Another approach described in Ref. [10] may deal with considerable values of PMD however, it requires high rate spectral analysis and it obtains spectral nulling of the signal in a very localized region that contains small amount of energy.

Preferred embodiments of the present invention

In order to overcome these limitations, methods and apparatus are disclosed. A temporal super resolving method allowing the estimation of high rate pulses using low rate electronic processing is disclosed. The approach is based upon a conversion of temporal degrees of freedom (temporal bit stream) into dynamic range readouts of the low rate detector. The technique may be successfully used for BER estimation and in-channel OSNR extraction where the position of the mapping points reveals the bit stream that was transmitted and the standard deviation around each point indicates the noise existing within the channel.

1

The disclosed approach is not used to recover the bit streams itself but rather to obtain the monitoring for the high rate incoming data.

Fig. 1 depicts the optical configuration used for the optical realization. According to the figure, the incoming signal is temporally gated, the filtered by a fixed filter (e.g., Bragg filter), and detected by a detector which can be a low rate electronic detector. At last the detected signals are processed by a DSP unit, which can also control the whole system.

The data stream is processed with low band electronics but with high dynamic range. The channel capacity equals to:

$$C = N \cdot \log_2(1+SNR) \tag{1}$$

Where N is the bandwidth product. In this disclosure, the $\log_2(1+SNR)$ factor is used in order to reduce the requirements from the temporal bandwidth of the channel (for SNR of 30db this factor equals to 10).

The low band electronics reduces the temporal resolution. This resolution is recovered by off line digital processing since the information is not really lost but converted to the dynamic range of the detectors. For instance, if a binary signal stream is passed through a Bragg narrow pass filter the readout is a combination of the various bits while each bit contributes a phase that is proportional to the position of the narrow pass band and the temporal distance of the bit from the origin:

$$A_m e^{i\phi} = \sum_n B_n e^{2\pi i(\delta v)n(\delta t)} \tag{2}$$

Where δv is the spectral distance between the optical carrier and the pass band of the filter and δt is the temporal resolution.

If the overall phase and the amplitude of the readout are measured, the value of the readout may be translated into the phase of each one of the components in the summation in Eq. (2). This phase is directly related to the existence of the various bits in the stream. This conversion is a one to one relation for instance in the case where the distance of each bit from the origin is increased by a power of 2. Then, the value of the phase of the readout is to be presented in binary base and the values of one and zeros in this representation are exactly the bits stream.

It is noted that there is a problem to measure the phase and the amplitude. One possibility to detect the phase is by using a Bragg filter having two symmetrical pass bands around the optical carrier frequency. In that case the temporal readout of the low band detector becomes:

$$A_m \cos(2\pi\delta vt + \phi) \tag{3}$$

Two readout couples were used to extract the amplitude and the phase of the expression in Eq. (3). The output was sampled twice with a constant time delay between samples of 0.6 nsec. The two normalized readouts of the detector are denoted v_1 and v_2 and they were used as the horizontal and vertical axes in all the figures.

The simulation of **Fig. 2** depicts one step of the one to one conversion of the bit stream into amplitude A_m and a phase for a sequence of 6 bits (64 possibilities) with a symmetric pass bands position of $\delta v = 1.67Ghz$ (for a stream rate of 10Ghz)

which is equivalent to $2\pi\delta v\delta t = 0.33\pi$. The width of the narrow pass band filter for this case was 900Mhz. Each of the axes in the figure is one readout of the detector, measured in Volts (normalized to maximum) and at a constant time delay between the two measures. Any such two readouts couples were measured for a specific sequence of 6 bits. The readouts are denoted v_1 and v_2.

Fig. 3 Computer simulations for optimizing the spectral bandwidth of the filter. This figure is based on plots such as Fig. 2 of v_1 and v_2, where the width of the band pass filter (x axis, in MHz) were changed per each such plot. Per each such plot, the smallest distance between any two points on the plot was found (y axis, dimensionless).
Obviously, for proper discrimination one wishes to have this smallest distance as large as possible. From the figure it is appears that, in these specific results, around 900Mhz there is an optimal working point.

Experimental Validation

     Figs. 4 present a statistical simulation that investigates the performance of the technique of **Fig. 2**, in a presence of white ASE noise and energetic fluctuations of the bits stream energy. **Table 1** summarizes the visual results depicted in **Fig. 4**. In table 1 one may see the values for the standard deviation of the 100Ghz ASE noise and the standard deviation for the amplitude variations of the signal. For both distributions a Gaussian distribution was assumed. Note that the 100Ghz bandwidth ASE standard deviation may be related to the OSNR according to the following ratio:

$$\sigma = 10^{-\frac{OSNR}{20}-0.5} \qquad (4)$$

In Table 1 the simulated noises include the standard deviation of the ASE noise and the standard deviation of the amplitude fluctuations of the signal. σ_1 and σ_2 are the standard deviation of the two closest points in the readout plane, respectively (obtained over more than 100 ensembles). Distance parameter is the distance between the two closest points in the readout plane. In **Fig. 4d** the effect of chromatic dispersion with Dz=1[ns/nm] was simulated. As one may see the effect of dispersion on the position and the standard deviation of the mapping points is week.

Fig. 4: Sub-figure number	ASE Noise	Amplitude Noise	Distance	σ_1	σ_2
a	-23dB	0	-0.003	0.003	0.003
b	0	0.5 %	-0.004	0.003	0.0034
c	-23dB	0.5 %	-0.011	0.0044	0.0046
d	Dispersion Dz=1[ns/nm]				

Table 1: Summary of the obtained results depicted in Figs. 4.

     As seen from Fig. 4, the position of the mapping points reveals the bit stream that was transmitted. The standard deviation around each point indicates the noise

existing within the channel and thus it may be used for in-channel OSNR and BER extractions.

It is noted that even in the perfect case when no noise is present, the dynamic range required from the detector for 6 bits improvement (6 times improvement) should be $10 \log(2^{6bit}) = 18dB$.

Since the spectral narrow band pass filter has a narrow spectral response (a long temporal response) one needs to gate (temporally) the incoming bits stream prior to its input into the spectral Bragg filter. This gating is required in order to avoid the aliasing. The temporal window may easily be realized with an electro-optical absorption component. A slow electrical driver whose speed is also adapted to the bandwidth of the detector drives this device. If is for instance the spectral width of the band pass is 900Mhz and the super resolution allows using an electronics of 1.67Ghz (6 bits super resolving), then the duty cycle of the gating will be:

$$DutyCycle = \frac{900Mhz}{1.67Ghz} = 54\% \tag{5}$$

Thus the overall time for computing the BER/in–channel OSNR will be increased by a factor of less than 2 (1/0.54). The signal detected by the detector is processed by the DSP in order to obtain the resulted parameters. The DSP unit can also comprise a control unit for the whole system.

It is noted that the fact the duty cycle is not 100% is taken as advantage in the reduction of the sampling rate of the detector: As previously mentioned in order to perform the mapping, two intensity readouts are required. The readouts are done in such a manner so that there is no more that one sample in a temporal period of 1/1.67Ghz.

Note also that the shutter is realized in order to prevent from the temporal response of the fixed optical filter to interfere with the adjunct 6-bit sequence. Since the spectral width of the filter is 900Mhz, the shutter per each bit stream realizes a temporal window of 1/900Mhz. This may be done only if the inverse Fourier transform of the optical filter does not generate temporal side lobes exceeding the temporal slot of 1/900Mhz. To assure that, the optical filter may have a shape of a Kaiser window that is a function whose inverse Fourier transform exhibits very reduced side lobes. The Kaiser window previously mentioned may be expressed as:

$$w[n] = \frac{I_0 \left[\beta \sqrt{1 - \left(\frac{n - \alpha}{\alpha} \right)} \right]}{I_0(\beta)} \tag{6}$$

Where I_0 is the zero order modified Bessel function and α, β are parameters of the window.

In order to realize a low price gating electronics, two effects will be examined. First the influence of a gating response that has response transients corresponding to less than 2.5Ghz. The second effect is the influence of the jitter obtained due to the fact that the electronics is low rate electronics. The first effect yields a good one to one conversion between the bit stream sequence and the measured parameters in the detector. Regarding the jitter, it is common to assume a jitter of few psec as typical in

4

this type of low rate circuits. Since the bits are in 10Ghz (100psec periods) few psec of jitter mean a mistake of few percents in the energetic fluctuations. The simulation presented in **Fig. 5** depicts the drift of the points obtained in the detector readout plane as function of the jitter while an exponential envelope was assumed to simulate the first effect. The jitter between each two adjacent point in **Fig. 5a** equals to 10psec (10% from the pulse width). **Figs. 5b and c** present the readout mapping obtained for a single relative shift between the bits stream and the detection of 0% and 50% respectively, while the exponential envelop is taken into account. For both cases the one to one conversion is reserved. From **Fig. 5a** one may conclude that an overall jittering range of up to 20% yet allows differentiating between the various mapping points. Since in our case the jitter is only few percentages, the low rate (and low price) gating electronics will do.

It is noted that the meaning of this result is that the jitter should be less than 20% but no synchronization is required between the optical bits stream and the detection circuit.

According to another embodiment of the invention, a method and apparatus for in-channel OSNR estimation is disclosed. It is based upon periodic polarization encoding of the incoming bit stream that results in spectral nulling of the signal and not the noise in a pre-designed wide spectral band.

By knowing the OSNR within the WDM channel, the BER can be extracted. Assuming Gaussian distributions for the noises one obtains that:

$$\text{BER} = v_{inf} \frac{\text{erfc}\left(\dfrac{\text{OSNR}}{\sqrt{2}}\right)}{2} = v_{inf} \frac{\text{erfc}\left(\dfrac{I}{\sqrt{2}\sigma_I}\right)}{2} \tag{6}$$

Where I is the current in the detector, σ_I is the standard deviation of the current and v_{inf} is the carrier frequency of the information.

There are several noise sources that influence σ_I. One important source is the shot noise that is created in the detector due to the fact that the photons carry discrete quanta of energy. The standard variation of the shot noise is proportional to the square root of the number of the incoming photons.

$$\sigma_{ShotNoise} \propto \sqrt{\frac{\eta \cdot P_{in} \Delta t \lambda}{hc}} \tag{7}$$

Where P_{in} is the power of the optical signal, η is the percentage of the input power that is siphoned away for monitoring purpose, h is Plank constant, c is the velocity of light and λ is the average wavelength (considered 1550nm in this embodiment, however, can be any other relevant wavelength). Δt is the integration period. This noise is thus very affected by the power of the input signal. Since the signal is proportional to the number of photons, the signal to noise ratio will also be proportional to the square root of the photons number:

$$\text{SNR} \propto \sqrt{\frac{\eta \cdot P_{in} \Delta t \lambda}{hc}} \tag{8}$$

The ASE is the noise generated due to the amplified spontaneous emission of the amplifiers in the optical network. The standard deviation is related to the OSNR according to:

$$\sigma_n = 10^{\frac{OSNR}{20}} \qquad (9)$$

The noise may be modeled as a white Gaussian noise. Due to the fact that we have averaged several bits the standard deviation is reduced as follows:

$$\sigma_{\bar{n}}^2 = \frac{\sigma_n^2}{\Delta t \cdot v_{inf}} \qquad (10)$$

Polarization Encoding

According to a preferred embodiment of the invention, the system used for realizing the described method is shown in **Fig. 6A**. The incoming signal length (i.e., the length of the bits stream) is determined by a shutter. Then, a tapped delay line or a fabry perot resonator, is used to replicate the bit sequence and delay each replica with respect to other replicas; each replica is then polarized in such a way as to be encoded. The sequences are detected by the detector and post processed by the DSP in order to extract the needed parameters according to the described method. The DSP unit can also include a control unit for the whole system.

For clarity, **Fig. 6B** shows the pulse terminology used in this application, i.e., the pulse is composed of a signal part (P and S polarization states) and a PMD part (either P or S states).

The concept of the method is to generate a filter that is created by having various delays between the incoming sequences while each delay is multiplied by a different temporally varied coefficient realized due to the polarization encoding. This polarization-encoding coefficient is seen as a certain pattern for the signal or as approximately constant pattern for the PMD part of the stream while for the noise it is a random pattern. Thus, the noise is not affected by the spectral filter while the signal and the PMD are. The filter is responsible to zero a predefined spectral region allowing extracting the OSNR. The filter which is synthesize according to this invention is related to the coefficients of each sequence that are controlled by the polarization controller. The coefficients which are realized are samples of a Kaiser window.

It is assumed that by placing a tapped delay line or by using a Fabry-Perot resonator with low Finesse (of e.g. 8 or 16) with respect to the relevant channel, the incoming bit stream will be replicated N times. The Fabry-Perot may be obtained by coating dielectric mirrors on the cleaved ends of a fiber having a length of few km.

By multiplying each delayed version by a different coefficient and having a different delay for it yields a realization of a spectral filter:

$$s_T(t) = \sum_{n=0}^{N-1} a_n s(t - n\Delta t)$$

$$S_T(v) = S(v)F(v) \qquad (11)$$

$$F(v) = \sum_{n=0}^{N-1} a_n \exp(2\pi i n \Delta t v)$$

6

Where s(t) is the bit stream, a_n are the coefficients. Capital letters designate the Fourier transform of the variable denoted by the letter. F is the generated filter.

According to a preferred embodiment of the present invention, a polarization controller (PC), will generate coefficients (a_n) following samples of the Kaiser function for the signal while the noise will 'see' random coefficients. According to another preferred embodiment, The PC can be even simplified by assuming it has a rotating polarizer followed by an electro-optical material and then additional rotating polarizer. **Fig. 7** describes a schematic structure of the simplified PC.

The Jones matrix describing the output obtained out of such a device is:

$$I = \begin{pmatrix} 1 & 0 \\ 0 & 0 \end{pmatrix} \begin{pmatrix} \cos\varphi_1 & -\sin\varphi_1 \\ \sin\varphi_1 & \cos\varphi_1 \end{pmatrix} \begin{pmatrix} e^{-i\Gamma/2} & 0 \\ 0 & e^{i\Gamma/2} \end{pmatrix} \begin{pmatrix} \cos\varphi_2 & \sin\varphi_2 \\ -\sin\varphi_2 & \cos\varphi_2 \end{pmatrix} \begin{pmatrix} P \\ S \end{pmatrix} \quad (12)$$

Where φ_1 and φ_2 are the time varying angles of the rotating polarizes and Γ is related to the voltage to be applied over the electro-optical material:

$$\Gamma = \frac{V}{V_\pi}\pi \quad (13)$$

V_π is the voltage required for a P to S polarization state rotation. The angles and the voltage were chosen such that if the input of the system is P=1/√2 and S=1/√2 (polarization at 45 degrees) then the output would give coefficients of a Kaiser of order 7 for the signal. For the noise, however, a random sequence of coefficients will be generated. Since the noise's state of polarization is random, due to the random change of the angles random coefficients will be obtained. In order to increase the randomality, the angles are varied not only between the sequences but also within each bit stream sequence.

However, when random modulation of angles is applied it was found by simulation that the P and the S components of the PMD part will also be modulated by random coefficients (it is noted that in this disclosure, the P and the S polarization states are generated due to the PMD while the P+S state is coined signal's polarization state). However, since the PMD contains the P polarization and the S polarization having a slight delayed between them, their overall effect is:

$$s_P(t) = \sum_n a_n(t-n\Delta t)s_p(t-n\Delta t) \quad s_s(t) = \sum_n [0.5-a_n(t-n\Delta t-\delta t)]\alpha s_p(t-n\Delta t-\delta t)$$

$$S_p(v) + S_s(v) = \alpha S_p(v)\sum_n 0.5\exp(-2\pi i n\Delta t v) + \sum_n \big(S_p(v)\otimes A_n(v)\big)\exp(-2\pi i n\Delta t v)[1-\alpha\exp(-2\pi i\delta t v)]$$

$$(14)$$

Where $\otimes$ denotes a convolution operation, δt corresponds to the bit length, α is a coefficient describing the energetic ratio between the P and the S polarization state, capital letters represent the Fourier transform. Note that since $\Delta t \gg \delta t$, assuming $\alpha=1$ Eq. 9 becomes:

$$S_p(v) + S_s(v) \approx S_p(v)\sum_n 0.5\exp(-2\pi i n\Delta t v) \quad (15)$$

It is shown that although the spectral filtering felt by the PMD component of the signal is much more attenuated than that felt by the noise, that equals to:

7

$$\sum_{n} \left(N(v) \otimes A_n(v) \right) \exp(-2\pi i n \Delta t v) \tag{16}$$

Where A_n is the Fourier of the temporal random variation of the coefficient, N is the Fourier of the noise.

Note that for the signal we chose the constant a_n coefficient to follow the Kaiser window pattern. Usually, the Kaiser amplitude modulation is used in order to reduce the spectral side lobes of signals. The Kaiser window may be mathematically be expressed as:

$$w[n] = \frac{I_0\left[\beta\sqrt{1-\left(\dfrac{n-\alpha}{\alpha}\right)}\right]}{I_0(\beta)} \tag{17}$$

Where I_0 is the zero order modified Bessel function and α, β are parameters of the window.

The present system was simulated with input signal as a sequence of 1000 bits at 10 GHz. The input signal was duplicated 8 times with a time delay of 0.7 nsec. Each duplicated and delayed sequence was multiplied by a different Kaiser coefficient where the coefficients were: a_0= 0.0059 a_1=0.1476 a_2=0.5367 a_3=0.9357 a_4=0.9357 a_5= 0.5367 a_6=0.1476 a_7=0.0059. We assume that the P+S polarization state of the signal is known so that the PC may modulate it properly. This knowledge may be obtained in a technique similar to polarization nulling, to be performed prior to the periodic polarization modulation (by applying such a command on the PC so that the output from the polarizer is minimal. Then, the P+S state of the signal equals to a state that is perpendicular to the polarizer and then inverse the polarization rotation effect of the PC.)

The angles and voltage were changed from sequence to sequence and also changed inside the sequence. The angles within each sequence were changed 8 times. The Kaiser window designed for the signal was β=7.

Fig. 8 presents the theoretical estimation for the filter that the signal, the PMD part and the noise may be affected from the spectrum. As depicted, the signal part is attenuated by a factor of approximately 1000 in the spectral range around the 0.7Ghz. The PMD exhibits spectrally a sinc function while the noise feels a random spectral distribution. Thus, in comparison to the PMD filter, the noise will be attenuated approximately 5 times less. An optimization of those numbers may be obtained by using a more sophisticated PC.

Fig. 9a The coefficients felt by the signal and the PMD. a) Within a sequence. b) Within a bit. x-axis is in sec, and y axis is the intensity normalized to maximum.

The statistical results obtained using real Return to Zero (RZ) signals simulation is seen in **Fig. 10**. **Fig. 10a** is the spectral filter felt by the PMD (as expected by the theory, it is a sinc function). **Fig. 10b** presents the filter of the noise. Indeed it is much moiré random than the PMD and the ratio between its value for 0.7Ghz and 1.4Ghz is

5 times better than for the PMD. **Fig. 10c** is the filter of the signal. Indeed a Fourier transform of 8 terms Kaiser window.

It is noted that in the figures above a 10% PMD was assumed. Based on the parameters used for the simulation, the PMD attenuation is 5 times more than the one of the noise and the signal attenuation is 1000 more. A chart describing the expected measured OSNR as function of the true OSNR and the PMD can be plotted. The formula to be used is as follows:

$$OSNR_{Measured} = \frac{OSNR_{True}}{1 + \frac{I_\Delta}{I} OSNR_{True}} \quad (18)$$

Where I_Δ is the standard deviation of the power not due to the ASE noise but due to measurement mistakes and I is the signal average value. The obtained results are depicted in **Fig. 11**.

According to the present invention, it was proven that the apparatus has the ability to attenuate the PMD part of the signal stronger than the noise. According to another preferred embodiment, the apparatus can be improved, for instance, instead of one electro-optical material and two rotating polarizers two electro-optical materials and three rotating polarizers, can be used.

References

1. S. Nogiwa, et al, "Highly sensitive and time resolving optical sampling system using thin PPLN crystal," *Electron. Lett,* 36, 1727-1728 (2000).
2. L. A. Jiang et al., "Sampling pulses with semiconductor optical amplifier," *IEEE Journal of Quantum Electronics*, 37, 118-126 (2001).
3. R. Trebino et al., "Measuring ultrashort laser pulses in the time-frequency domain using frequency-resolved optical gating," *Review of Scientific Instrumentations*, 68, 3277-3295 (1997).
4. C. Iaconis and I. A. Walmsley, "spectral phase interferometry for direct electric-field reconstruction of ultrashort optical pulses," *Optics Letters,* 23, 792-794 (1998).
5. F. Deveaux et al., "Simple measurement of other dispersion and on chirp parameter of intensity modulated light emitter," *J. Lightwave Technol.,* 11, 1937-1940 (1993).
6. R. Monnard et al. "Real time dynamic chirp measurements of optical signal," OFC 1998, WC7.
7. Shake and H. Takara, "Flexible performance monitoring using amplitude histogram method in optical fiber communication," OECC, 570-571 (2002).
8. D. K. Jung, C. H. Kim, and Y. C. Chung, "OSNR monitoring technique using polarization-nulling method," *Optical Fiber Conf. '2000 Tech. Dig,* Baltimore, MD, Mar. 2000, paper WK4-2
9. J. H. Lee and Y. C. Chung, "An improved OSNR monitoring technique based on polarization-nulling method," *Optical Fiber Conf. '2001 Tech. Dig,* Anaheim, CA, Mar. 2001, paper TuP6
10. C. J. Youn, K. J. Park, J. H. Lee and Y. C. Chung, "OSNR monitoring technique based on orthogonal delayed-homodyne method," *Optical Fiber Conf. '2002 Tech. Dig,* Anaheim, CA, Mar. 2002.

What is claimed is:

1. An apparatus for in-channel optical signal to noise ratio estimation, comprising:
   - A shutter to determine the length of bit sequence;
   - A tapped delay line to replicate said bit sequence and delay each replica with respect to other replicas;
   - Polarization encoder to encode each said delayed bit sequence, and
   - A detector to detect said sequences

For the applicant,

Fenster & Co. Patent Attorneys, Ltd.
c:298/03282

Figures
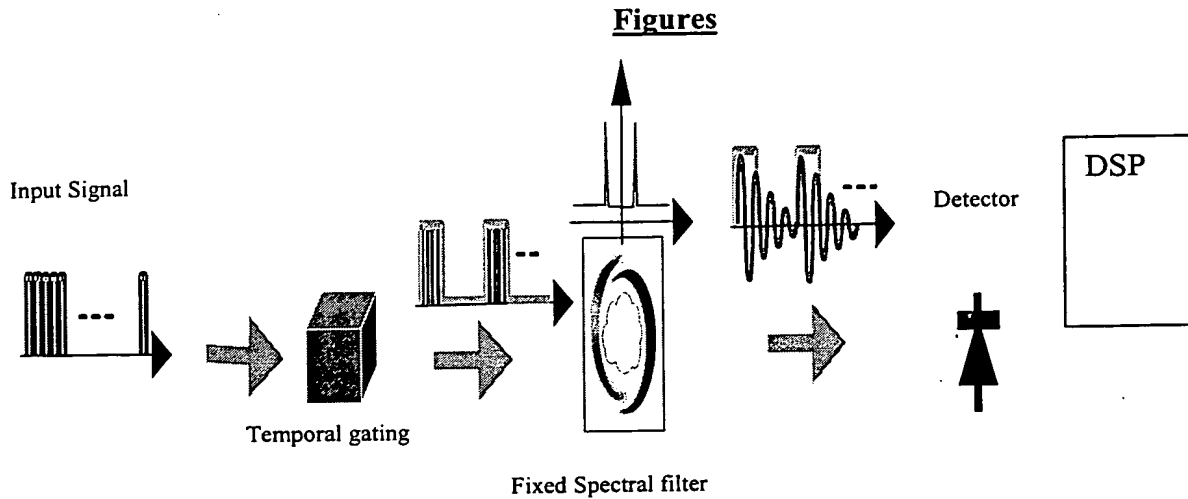
Fig. 1: The optical configuration of the apparatus.
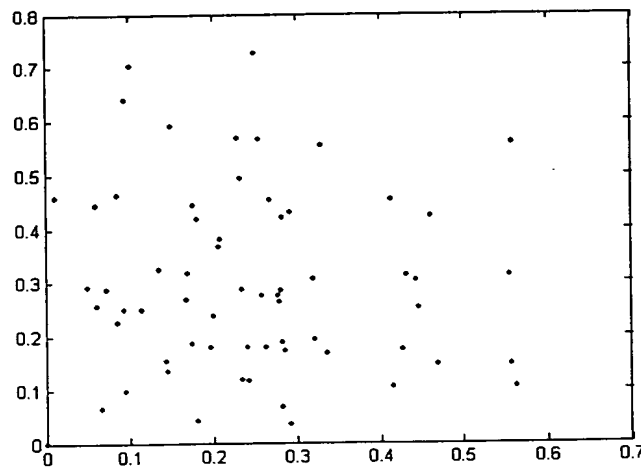
Fig. 2: Computer simulations which depict one step of the one to one conversion of the bit stream into amplitude A_m and a phase for a sequence of 6 bits (64 possibilities) with a symmetric pass bands position of $\delta v = 1.67 Ghz$ (for a stream rate of 10Ghz) which is equivalent to $2\pi\delta v\delta t = 0.33\pi$. The width of the narrow pass band filter for this case was 900Mhz. Each of the axes in the figure is one readout of the detector, measured in Volts (normalized to maximum) and at a constant time delay between the two measures. Any such two readouts couples were measured for a specific sequence of 6 bits. The readouts are denoted v_1 and v_2.

Fig. 3: Computer simulations for optimizing the spectral bandwidth of the filter. This figure is based on plots such as Fig. 2, where the width of the band pass filter (x axis, in MHz) were changed per each such plot. Per each such plot, the smallest distance between any two points on the plot was found (y axis, dimensionless).
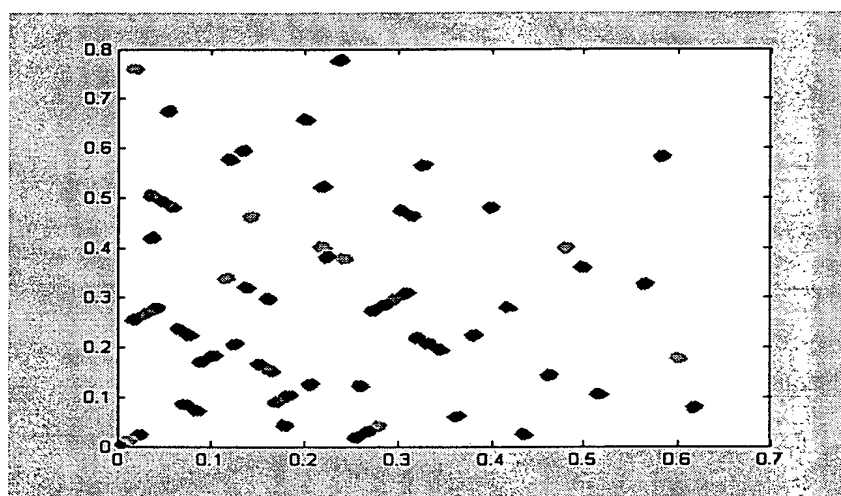
4(a)
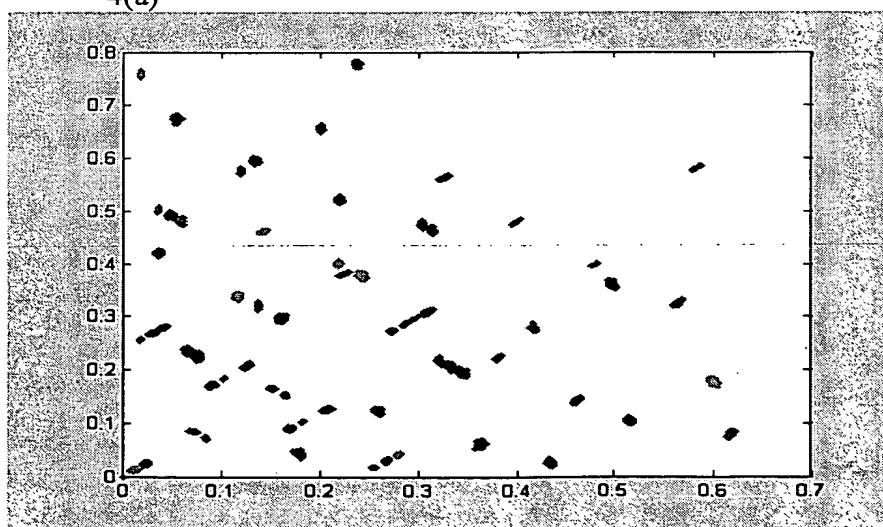
4(b)
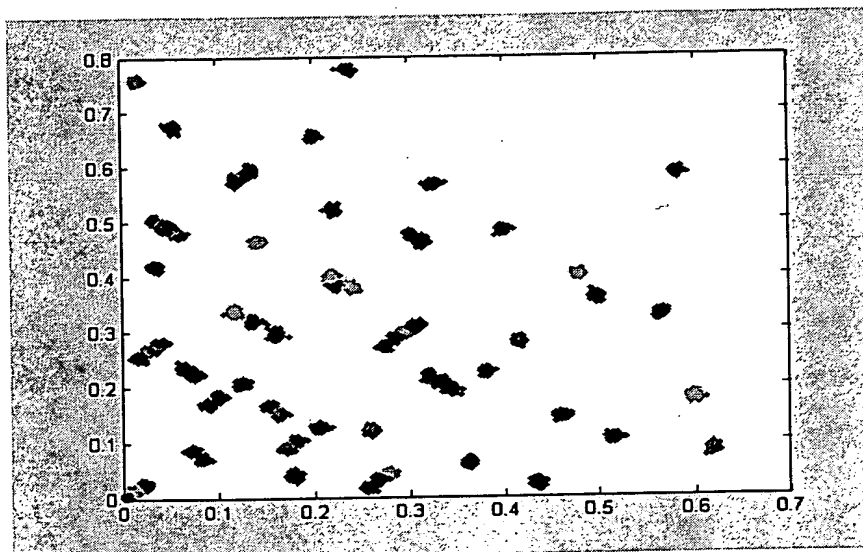
4(c)
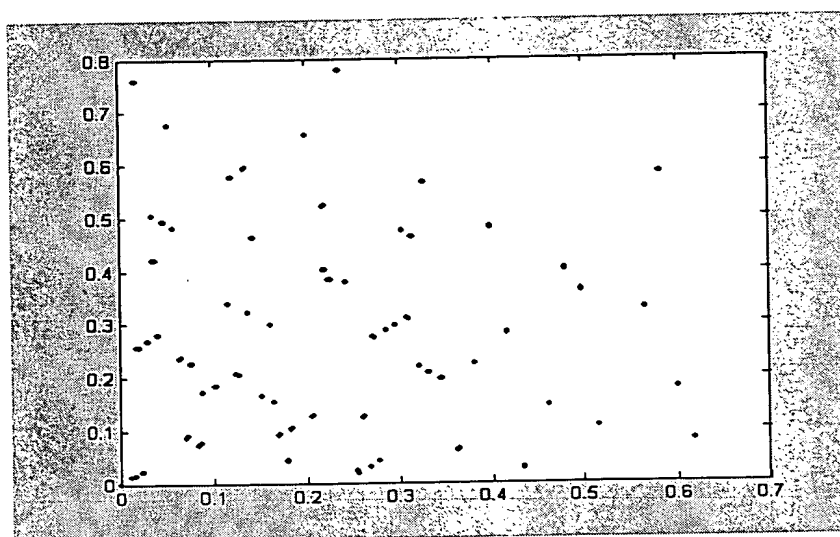
4(d)

Figs. 4: Computer simulations for the detection of bits stream sequences for various parameters of noise and energetic fluctuations. The same legend as of Fig. 2 applies here, however, for each figure (a-d), different parameters of ASE and amplitude noises and dispersion (according to Table 1) were applied.
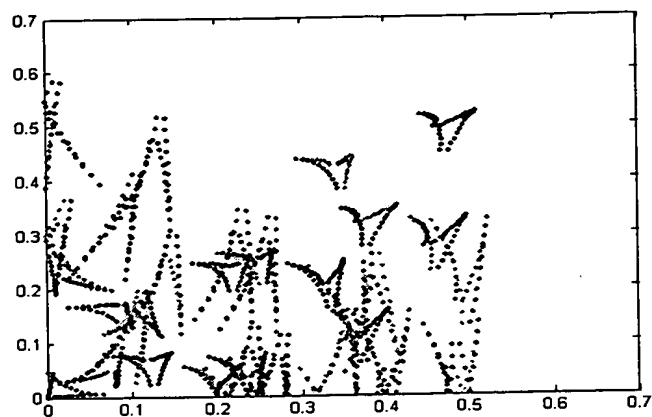
5(a)
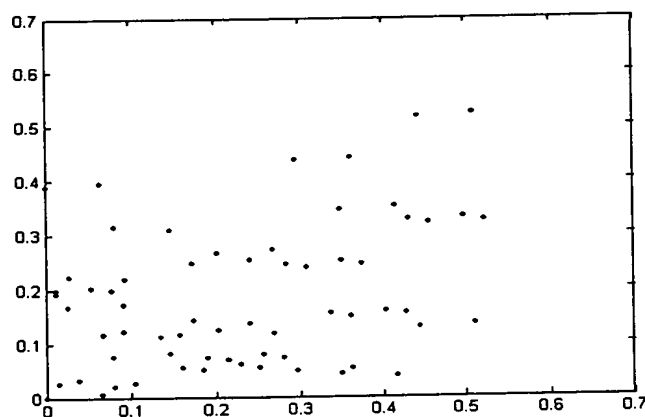
5(b)
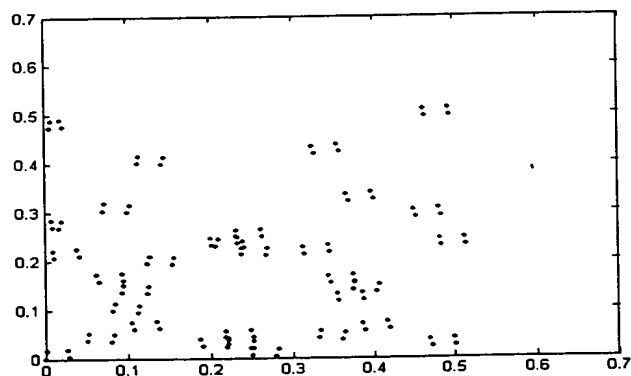
5(c)

Fig. 5: Temporal Gating circuit requirements. The same legend as of Fig. 2 applies here, however, for each figure, a different relative shift between the on-set of the gate and the time at which the first bit is received at the detector (jitter). a). jitter of 0% to 90% with steps of 10 % b). Relative shift of 0%. c). Relative shift of 50%.

Tapped delay line/

Fabry -Perot resonator

Detector

DSP

Incoming Signal

Shutter

Polarization
Encoder
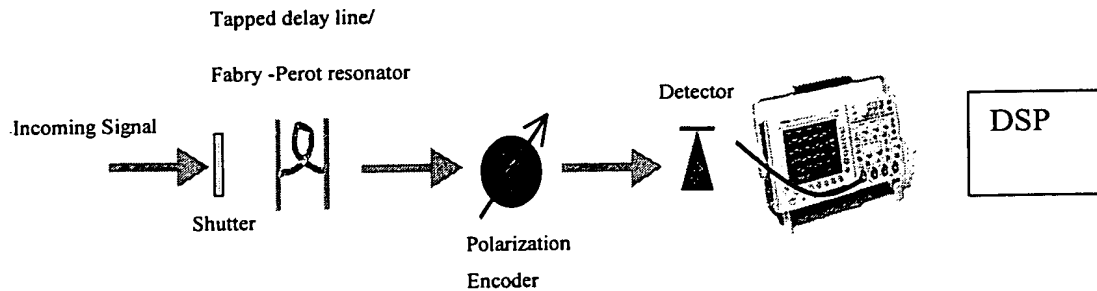
Fig. 6A: Schematic setup of the system

P state   P+S state   S state
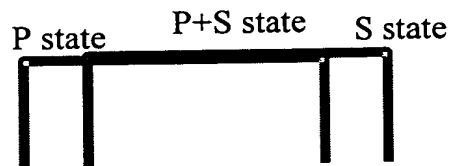
Fig. 6B: schematic representation of a PMD distorted pulse. It contains two parts – the signal (where both P and S polarizations exist, denoted P+S) and the PMD part (where either P or S polarization states exist.

E-O Material

P

S

Rotating
Polarizer

Rotating
Polarizer
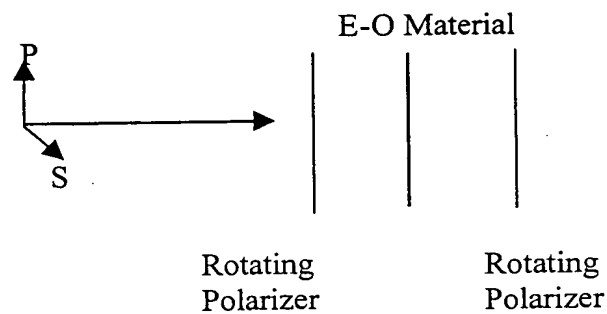
Fig. 7: Schematic structure of the simplified PC (E-O stands for Electro-Optical).
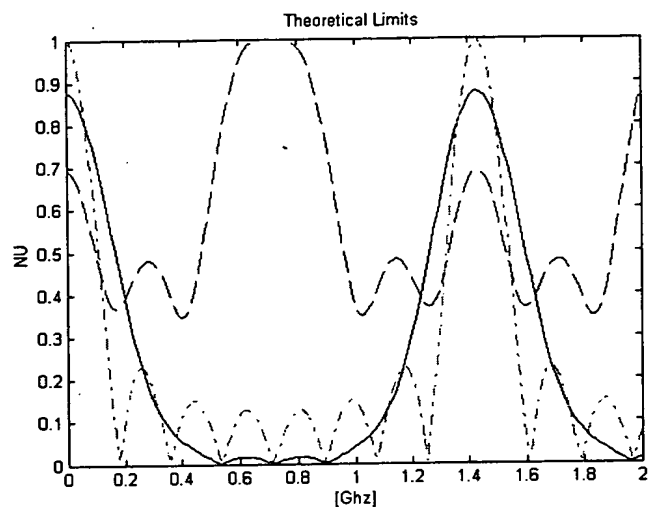
Fig. 8: The theoretical limits of the approach. The obtained spectral filter for the signal (solid line), the noise (dashed line) and the PMD part (the dash doted curve). The y-axis is the filter transmittance and the x-axis is it frequency in GHz.
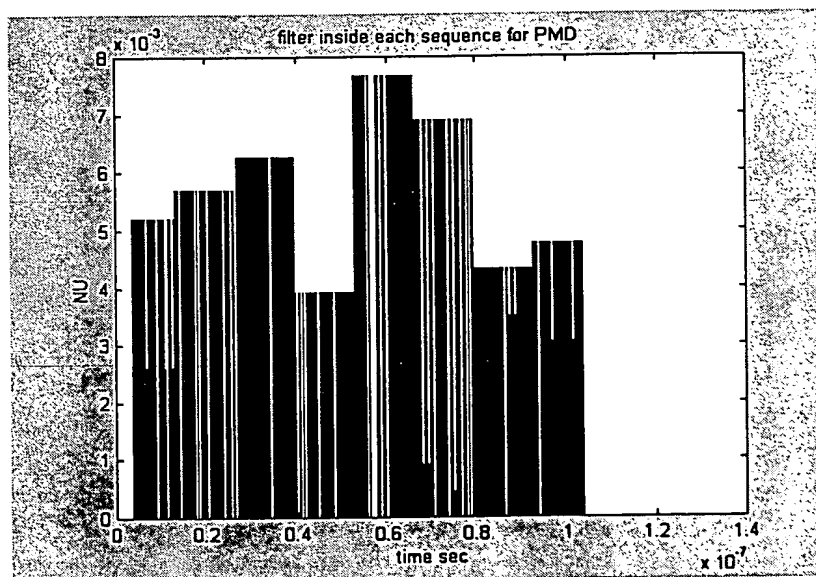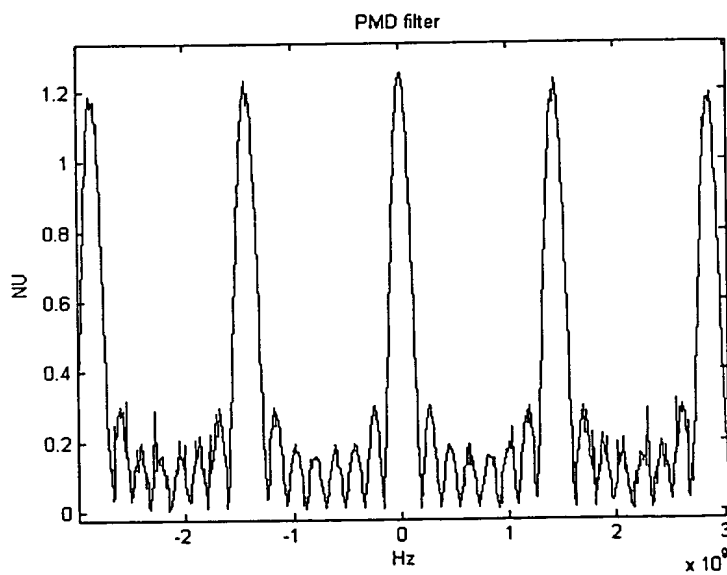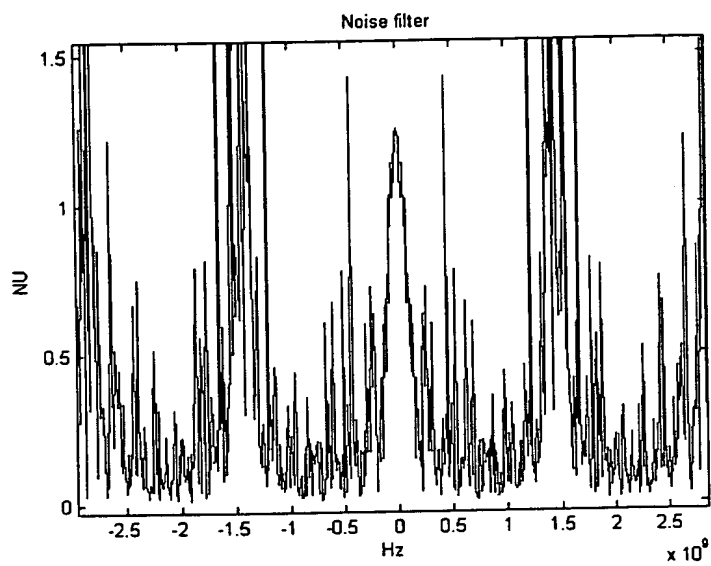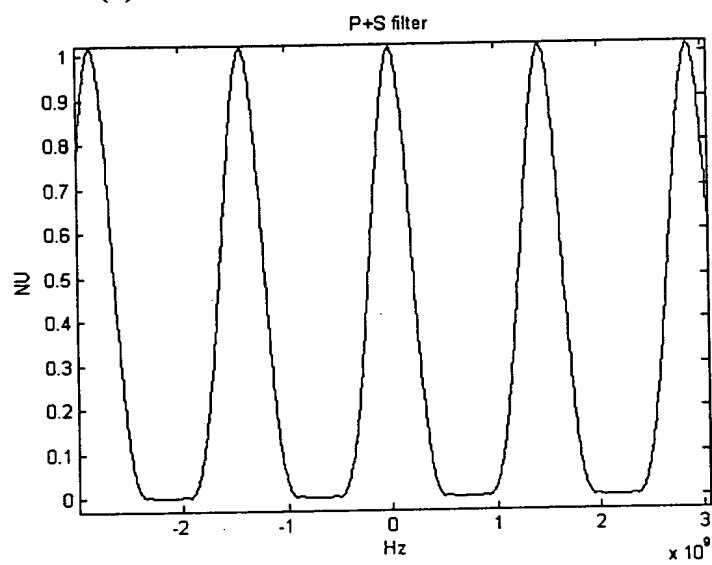

9(a)
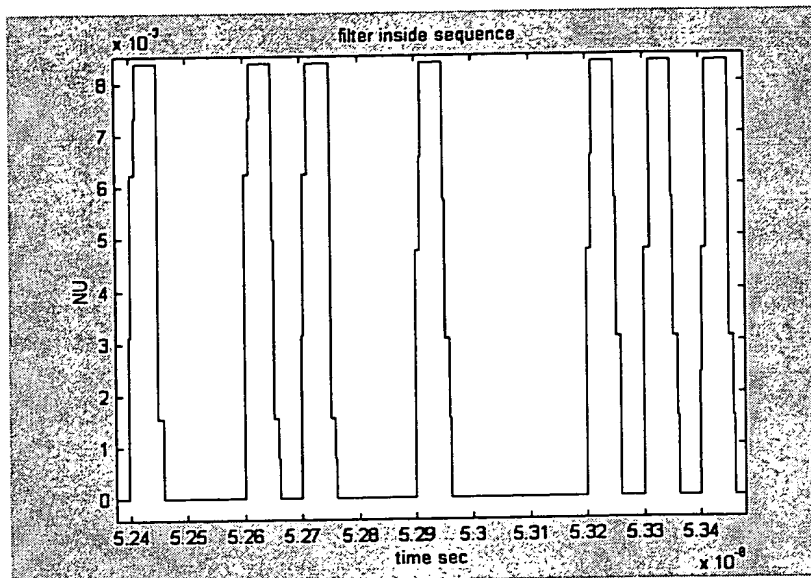
9(b)

Fig. 9: The coefficinents felt by the signal and the PMD. a) Within a sequence. b) Within a bit. x-axis is in sec, and y-axis is the intensity normalized to maximum.
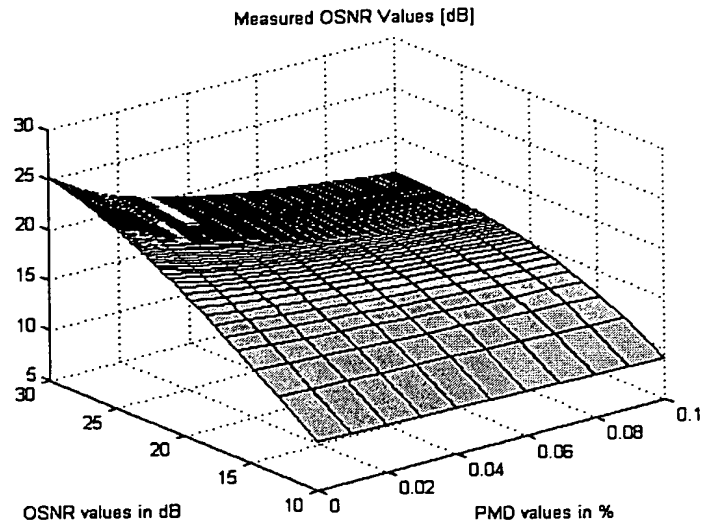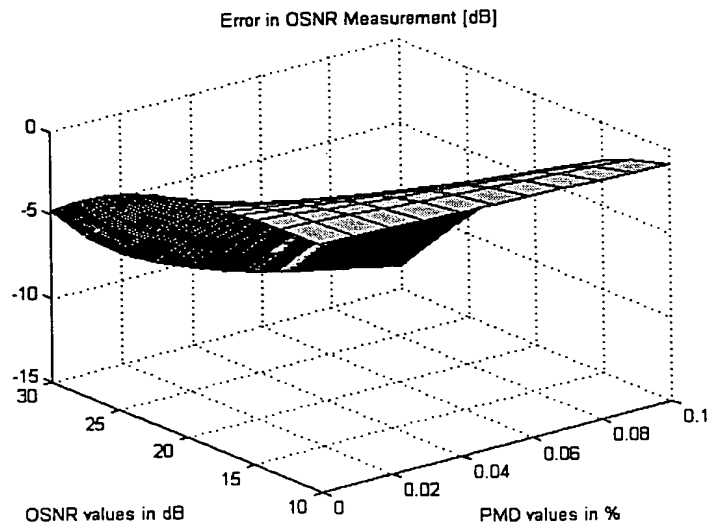

10(a)

10(b)

10(c)

Fig. 10: Experimental results. a). The filter of the PMD. B). The filter of the noise. C). The filter of the signal. X axis is the frequency in Hz and y axis the filter's transmittance.

Measured OSNR Values [dB]

11(a)

Error in OSNR Measurement [dB]

11(b)

Fig. 11: The simulation for the precision obtained in the in-channel OSNR measurement.
a). The measured OSNR vs. PMD. b). The error between the measured and the true OSNR
vs. PMD.